CFD analysis flow through cryogenic expansion turbine ⊘

N. Srinivasa Rajneesh ✉ ; C. H. Ashok Kumar; Manish Sharma; Subramanyam Pavuluri

Check for updates

View Online   Export Citation   CrossMark

22 November 2023 17:45:29

CFD Analysis Flow Through Cryogenic Expansion Turbine

N. Srinivasa Rajneesh [a), CH. Ashok Kumar [b), Manish Sharma [c), Subramanyam Pavuluri [d)

Department of Mechanical Engineering, Malla Reddy Engineering College, Secunderabad, Telangana State, India

[a) *Corresponding author: rajneeshsrinivasa@gmail.com*
[b)*chashok027@gmail.com*
[c)*manish.mvs@gmail.com*
[d)*subramanyampavuluri@gmail.com*

Abstract—Analysis of flow via the cryogenic expansion turbine using computational fluid dynamics. The flow through an expansion turbine with radial input and axial exit must be analysed in three dimensions. ANSYS Blade Gen, ANSYS Turbo Grid, and ANSYS CFX are the tools used in this process. ANSYS BladeGen was used to build the turbine's 3D model. ANSYS TurboGrid generates the mesh and ANSYS CFX does the analysis. Cryogenic turbine flow is first modelled using data, then meshes are created, and various velocity and pressure contours are drawn to study the flow.

Keywords— ANSYS Blade Gen, ANSYS Turbo Grid and ANSYS CFX, Cryogenic expansion turbine

INTRODUCTION

While the earth's atmosphere (oxygen, nitrogen) and the crust (natural gas, helium) are teeming with gaseous raw materials, we must harness and store them in order to put them to good use. Industrial gases such as oxygen, nitrogen, helium, and argon are essential. Helium, argon, and other noble gases may be found in the earth's crust, as can oxygen and nitrogen from the atmosphere. The primary goal is to employ these gases in a significant way. The economy is heavily reliant on the production and use of these gases. Steel production, rocket propulsion, and medicinal usage all rely on oxygen [1-2].

TIG welding and high temperature furnaces utilize argon. Superconductivity, nuclear reactors, and other applications need for helium. Rocket propulsion systems utilize hydrogen as a fuel. The fertilizer business relies heavily on nitrogen. Additionally, it is used in the fields of cryosurgery and the semiconductor manufacturing process. Chemical operations rely on nitrogen as a blanket gas and as a raw ingredient for ammonia-based fertilizers and chemicals. Shrink suited to cryosurgery, liquid nitrogen is the most efficient chilling medium, and high purity nitrogen is used as a carrier gas in the electronic industry [3-4].

Air separation is the first step in the process of separating the gases. Expanding turbines are used to divide the air. Several factors contribute to turbo expanders' superiority over high-pressure air separation (Linde). Product variety and operational flexibility are all included in this bundle. It's still cryogenic distillation that's used to make bulk industrial gases, even while adsorption and membrane separation processes at the upper temperatures gain popularity. When compared to conventional room-temperature distillation, the use of cryogenic distillation, which operates at temperatures below 100K, has several benefits. This technique may produce large amounts of argon and other rare gases, as well as liquid goods. Propane and other heavy hydrocarbons are removed from natural gas using turbo expanders [5-7].

Turbospreaders ethane recovery requires low temperatures, which turbo expanders are able to provide at a lower cost. Refrigeration, high-pressure wellhead gas, geothermal heat power cycles, and pressure letdown are all possible uses for expansion turbines. Paper and other industries, as well as cryogenic process facilities, use expansion turbines for waste gas energy recovery [8]. Expansion turbines may last for years and are more dependable than reciprocating expanders. Gas lubricated bearings are maintained by process gas. This is made feasible by the process gas. In contrast, the input and discharge directions of cryogenic turbines are radial and axial, respectively.

The single stage expansion ratio of cryogenic turbines means that they are always single stage machines. It is also possible to use turbo-expanders to offer both cryogenic and ambient cooling. Closed-cycle Reversed It is possible to keep radiation detectors and superconducting magnets cool using Brayton cryo-coolers [9].

Other uses for turbo expanders include creating refrigeration for air conditioning in airplanes, as well as making liquid cryogens. An expansion turbine removes propane and other heavy hydrocarbons from natural gas streams. It's the most cost-effective way to get the low temperatures needed for ethane recovery [10].

Applications that extract energy, such as refrigeration.

- Electricity generated by high-pressure natural gas
- Thermoelectricity
- In cryogenic process facilities, the Organic Rankine cycle (ORC) is used to reduce total utility usage.
- For waste gas energy recovery in the paper and other sectors.
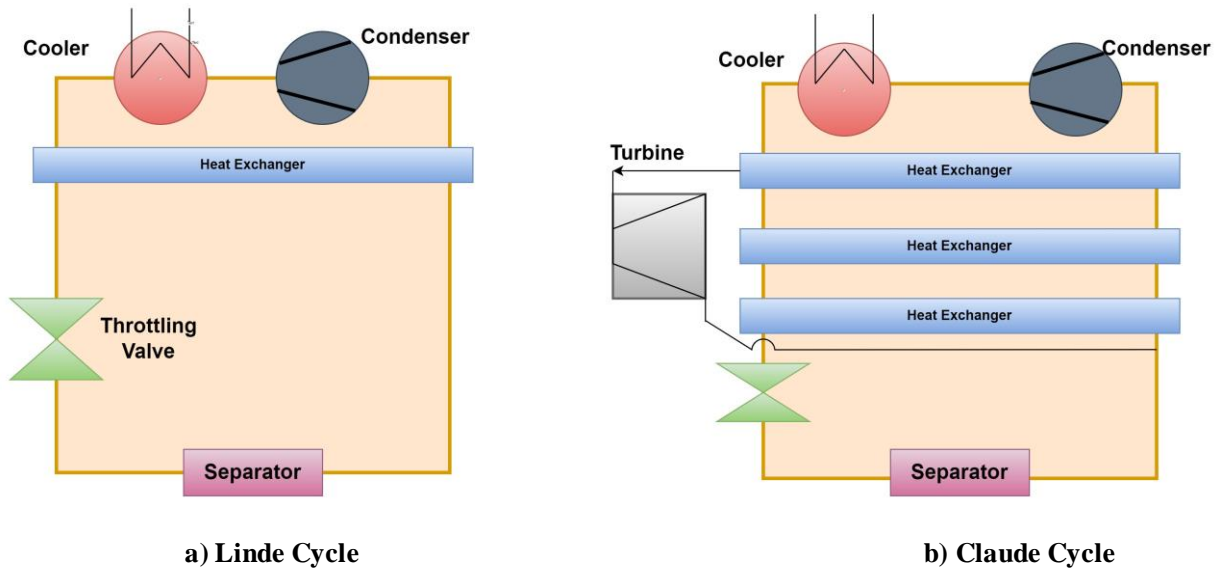- Impurities in gas streams may be frozen or condensed.

| a) Linde Cycle | b) Claude Cycle |

FIGURE 1. With and without active expansion devices in cryogenic refrigeration.

LITERATURE REVIEW

It is a wonderful resource for tiny cryogenic turboexpander development. Textbooks on cryogenics and turbomachinery are well-known. Scholar provides an overview of turboexpanders and their application in contemporary, cost-conscious industrial facilities. Lessons from Whitfield and Baines' performance analyses Studies on turboexpander technology may be found in major conference proceedings and periodicals like Advances in Cryogenic Engineering. 8-millimeter turbine from Boulder's National Bureau of Standards [11-12].

The turbine ran at 600,000 rpm at 30 K. Its cryogenic turboexpanders with gas bearings were invented in 1974. Cryostar, Switzerland, began developing an axial and radial cryogenic turboexpander in 1981. A miniaturized turboexpander for helium cooling was created [13]. The turboexpander's lower and higher ends had radial inward flow reaction turbines and centrifugal braking fans. 6mm turbine wheel, 4mm shaft the turboexpander's first and second stages spun at 816 and 519 kph. They collaborated with Goddard Space Flight Center on Brayton Cycle cryocoolers. MILLION RPM 1.5 mm DIAMETER TURBINE (rpm). The Chinese Academy of Sciences created a two-stage micro expansion turbine to generate 1.5 L/h helium. Their rpm was above 5,000,000. NBS USA has created a miniature turboexpander. The first expander ran at 600,000 rpm on gas bearings. MCH facilities in Moscow use Davydenkov et al's foil bearing turboexpander [14].

The rotor could reach 240,000 rpm and the shaft was 16 mm. "Cryogenmash" invented the turboexpander for the gas expansion machine regime in 1991. In their description of turboexpander design, Authors mention CFD software, CNC, and Holographic methods [15]. Another author built it for the Fermi particle accelerator's helium-liquefying equipment. A 4.76 mm turbine rotor and a 12.7 mm brake compressor held the shaft. A 384,000 rpm expander can cool 444 watts [16-17].

Author produced cryogenic turboexpanders with rotors up to 103 mm long and 0.9 N heavy. Both kinds of gas-lubricated foil journal bearings were tested on the turboexpander. By using active magnetic bearings instead of oil-

based systems, Atlas Copco has eliminated the need for [18-20] developed an inward flow radial turbine for cryogenics. India's research and development lags behind. In the last two decades, CMERI Durgapur has expanded dramatically. 40,000 RPM continuous rotation but the initiative failed to make any progress [21]. A turboexpander of 80,000 rpm was built by IIT Kharagpur. Dr. Ghosh's PhD dissertation focuses on cryogenic turboexpanders. For 20K, BARC's Cryogenic Technology Division has developed heated Helium refrigeration [22-23].

DESIGN OF EXPANSION TURBINE MODEL
Modelling the Blade Profile

An ANSYS BladeGen is used to build the model. It is a specialist geometry generation tool for turbine blades. Before processing, the blade surfaces are constructed, a solid model for the blades and hub is created, 2-D drawings are drawn for meridional contours and nonflow-path hub geometry, as well as periodic fluid zones are created. BladeGen's graphical user interface (GUI) is how it gets input from the user (GUI) [24].

ANSYS BladeGen

ANSYS BladeGen is used to build the blade profile, which is based on the dimensions provided in Fig. 2. Tie lines connect the hub and tip streamlines to form a governed surface. As a result, the surface formed is regarded as the blade's "mean surface." Solid and wireframe models of the BladeGen passage built using ANSYS BladeGen's Blade profile are shown in Fig. 2 [25].
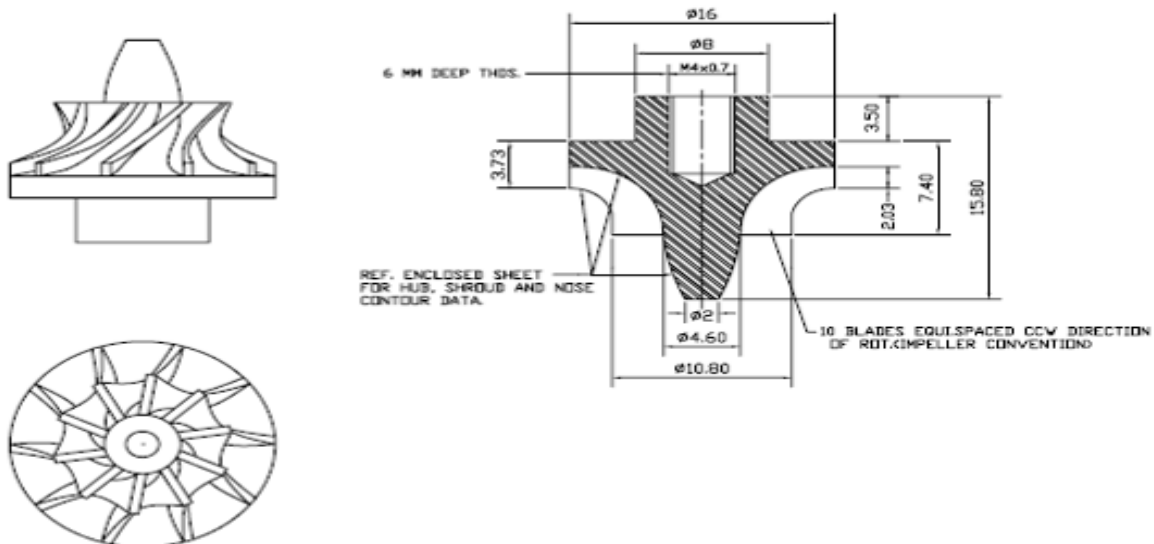
FIGURE 2. Turbine wheel

MESHED MODEL OF BLADE PROFILE

ANSYS TurboGrid

Analysts of rotating equipment utilize ANSYS TurboGrid, often known as mesh, to construct high-quality hexahedral meshes, while keeping the underlying geometry of the system. In the ANSYS process, these meshes are utilized to tackle difficult blade passage issues. H/J/C/L- Grid is a suitable architecture for inward radial turbines. As long as include O-Grid is checked, the mesh's orthogonality surrounding the blade will be improved. There are 3,46,122 nodes and 3,20,800 elements in ANSYS TurboGrid's total node count. Figure 3 shows an ANSYS TurboGrid meshed model of blade passage.
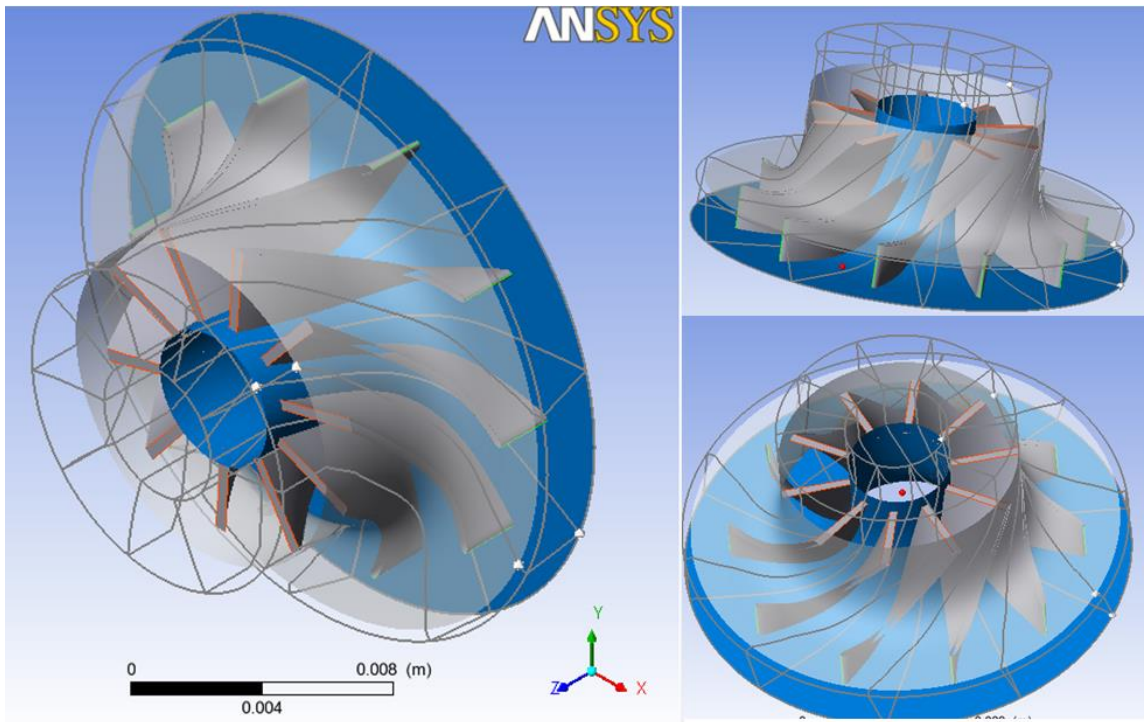
FIGURE 3. ANSYS TurboGrid

THE STRUCTURE OF ANSYS CFX

In order to do a CFD study, ANSYS CFX utilises four software modules that accept a geometry and mesh and send the necessary data to them.
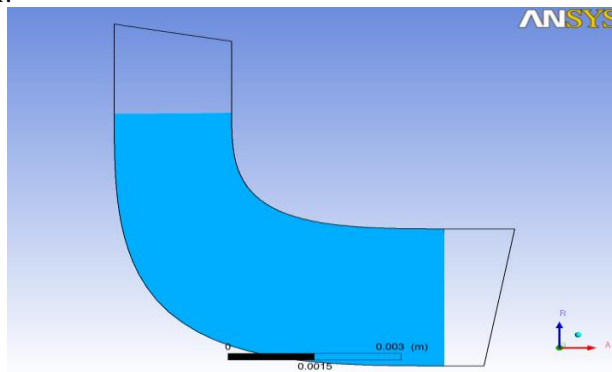

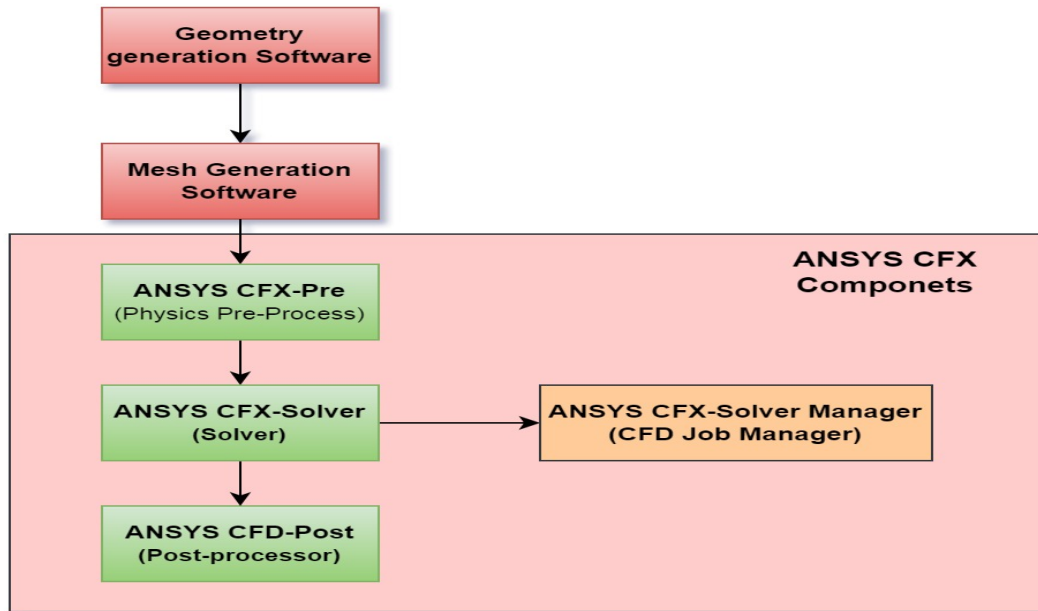**FIGURE 4.** Meridional View of the Blade, Hub and Shroud

FIGURE 5. The Structure of ANSYS CFX

DEFINING BOUNDARY CONDITIONS

Some of the topics covered include flow physics and solver parameters. Analyses. ANSYS CFX-Pre provides boundary conditions for heat transfer models and periodicity. To create simulations, the CFX-Pre physics pre-processor is used. It is possible to import many meshes, enabling the most suitable mesh to be used in each area of complicated geometries. To illustrate the turbine's boundaries, the pressures at the intake and output are depicted as constant in a table.

TABLE 1. Boundary conditions for five cases at Inlet and Outlet of Turbine

Inlet Pressure (bar)	Outlet Pressure (bar)	Inlet Temperature (K)	Outlet Temperature (K)
1.8	1.5	99.65	120
2.2	1.5	99.65	96
2.9	1.5	99.65	90.02
3.3	1.5	99.65	85
3.6	1.5	99.65	80

ANSYS CFX-Solver

An issue specification's CFX-Solver solves all of its CFX-Pre-created simulation's solution variables. ANSYS CFX makes use of a connected solver to solve all of the hydrodynamic equations in one go. There are less iterations with the linked solver than with the standard segregated solver for a convergent flow solution.

ANSYS CFD-Post

Interactive graphics tools for CFX simulation results are provided by CFD-Post, a state-of-the-art post-processing application.

RESULTS & DISCUSSION

Pressures at both the intake and outlet are kept constant throughout the analysis of five different pressures. To reduce the turbine's temperature and pressure output. Throughout the investigation, the discharge will be taken for granted. Various pressure heads were used in the investigation. Temperature, pressure, entropy, and velocity

contours were used to study the flow of entropy, pressure, velocity, and temperature across the blade passages. The turbine's efficiency is displayed at various pressure ratios.

Validation for Case 3

The CFD results of case 3 are validated with analytical values. It is observed from table 2 that the CFD values of the case 3 are in fair agreement with analytical values.

TABLE 2. Comparison of CFD values with Analytical values

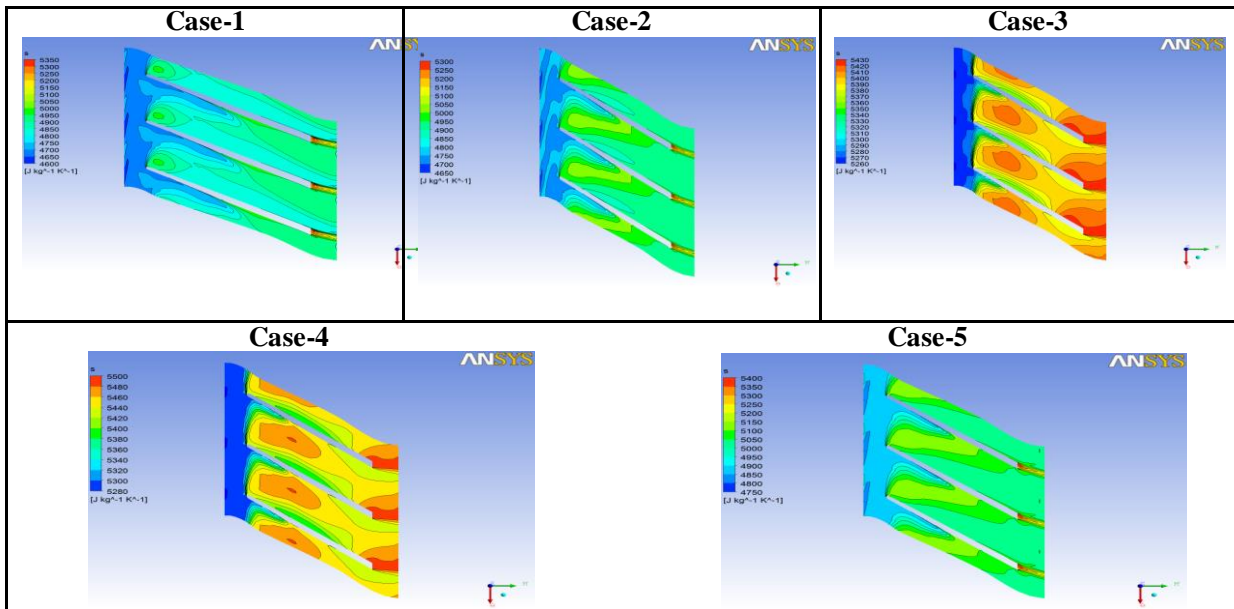|	**Analytical values**	**CFD values**
Inlet Pressure (bar)	2.9	3
Outlet Pressure (bar)	1.29	1.5
Inlet Temperature (K)	99.65	112
Outlet Temperature (K)	85.96	90
Inlet Entropy (kJ/kg.K)	5.352	5.36
Outlet Entropy (kJ/kg.K)	5.452	5.415
Inlet Velocity (m/s)	204.3	220
Outlet Velocity (m/s)	90.1	90

BLADE TO BLADE PLOT

FIGURE 6. Velocity Vectors at 80% Span

- Case 1 (fig. 6) shows a fluid input velocity of 220 m/s and an expansion turbine exhaust velocity of 160 m/s. Because the flow at the entry is cycled closer to the suction surface, eddies have formed.
- Instance 2 (fig. 6) shows a modest difference in input and exit velocities when compared to case 1.
- Case 3 (fig. 6) shows that the input fluid velocity is 220 m/s and the expansion turbine output fluid velocity is 80 m/s. Flow has been found to be circulated and replenished at the front door. At the turbine's outlet, the flow shifted to the suction side.
- Case 4 (fig. 6) shows that the input fluid velocity is 210 m/s and the expansion turbine exit fluid velocity is 60 m/s. Compared to scenario 5, the turbine's exit velocity drops by a quarter of a percent.
- Fig.4.1 shows that in the instance of case 5, fluid velocity at the intake is 220 m/s m/s and the exit velocity is 170 m/s.
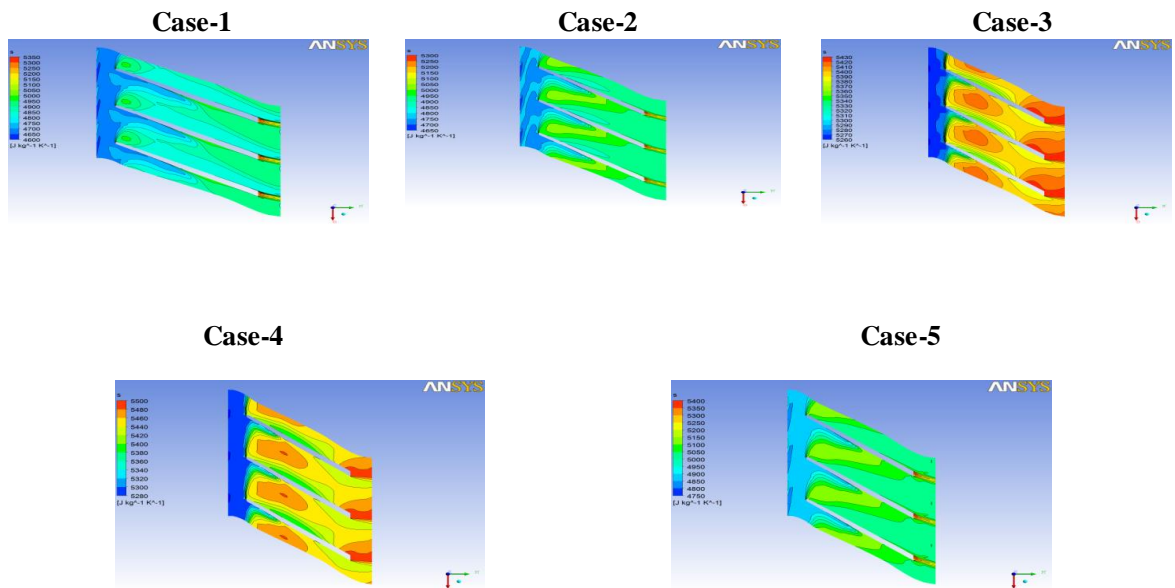
FIGURE 7. Contour of Entropy(s) at 80% Span

- There is a noticeable difference between the inlet and the exit entropy levels in example 1 (fig. 7). A blade's suction surface has an entropy maximum of 4850 J/kg.k at the entrance of the tunnel.
- Case 2 (fig. 7) shows an intake entropy of 4800 J/kg.k and an exit entropy of 4950 J/kg.k. 5100 J/kg.k. is the highest entropy at the blade passage's suction surface.
- Entropy at the intake is 5330 J/kg.k and at the exit is 5410 J/kg.k, as shown in figure 4.2. At 20 percent of blade passage from entry, entropy in the plane of blade to blade is 5420 J/kg.k at its greatest, while flow advance to exit steadily reduces in entropy.
- The entropy at the intake is 5320 J/kg.k and the entropy at the exit is 5460 J/kg.k, as shown in instance 4 (fig. 7). The entropy in the middle region of the blade-to-blade plane at 30 percent of the blade passage from the entrance is 5480 J/kg.k., according to the results.
- For example, in Case 5 (Fig. 7), the intake entropy was found to be 4900 J/kg.k whereas the exit was found to be 5100 J/kg.k. On the suction surface of the blade, the maximum entropy is 4850 J/kg.k.

Efficiency rises with pressure ratio up to a certain pressure ratio of design value, then declines as pressure ratio increases, according to computational efficiency values. All examples except Case 3 have an out-of-turbine pressure of 1.5 bar or less that declines with increasing intake pressure. This is because stagnation pressure downstream progressively diminishes as inlet pressure rises. Anywhere from intake to mid-stream, static pressure rises and then declines until it reaches turbine-exit pressure. However, in example 3 there is a tiny fluctuation in the streamwise static pressure. From the turbine's intake to the turbine's exit, the streamwise location's static entropy progressively rises, then somewhat reduces, then rises again. As with scenario 3, however, there is a tiny fluctuation in the streamwise static entropy.
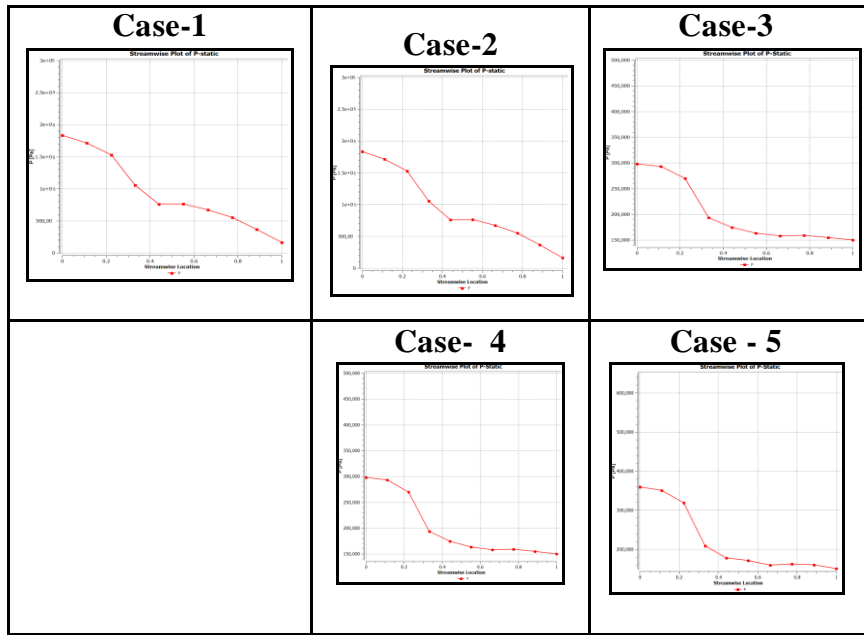
Case-1	Case-2	Case-3
	Case- 4	**Case - 5**

FIGURE 8. Streamwise Plot of P-Static

Case-1	Case-2	Case-3
	Case- 4	**Case - 5**
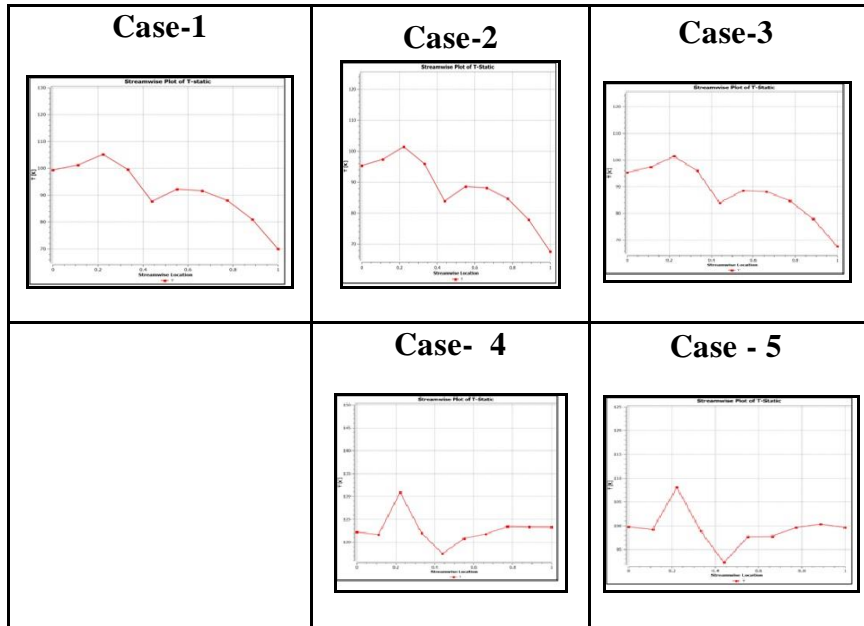
Figure 9. Streamwise Plot of T-Static

Case-1	Case-2	Case-3

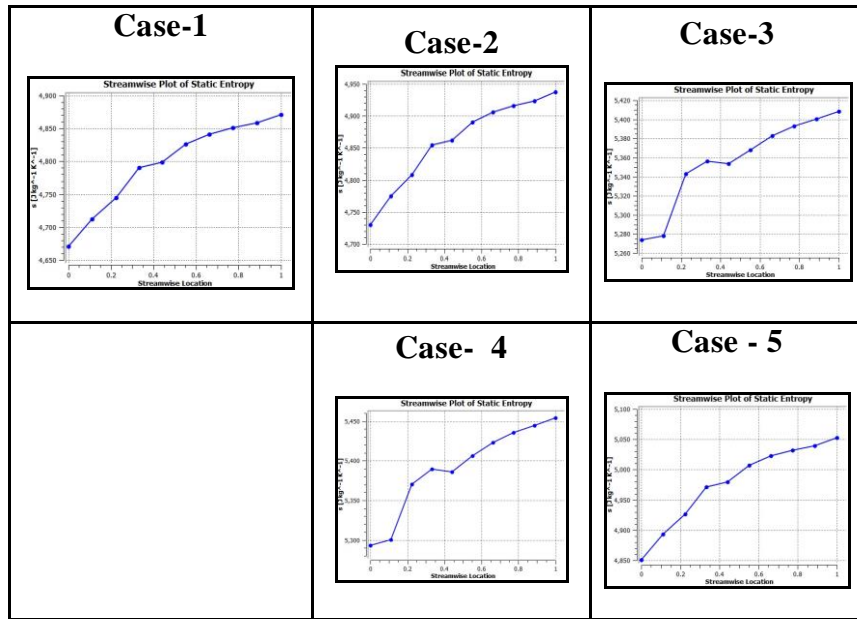|	Case- 4	Case - 5

Figure 10. Streamwise Plot of Static Entropy

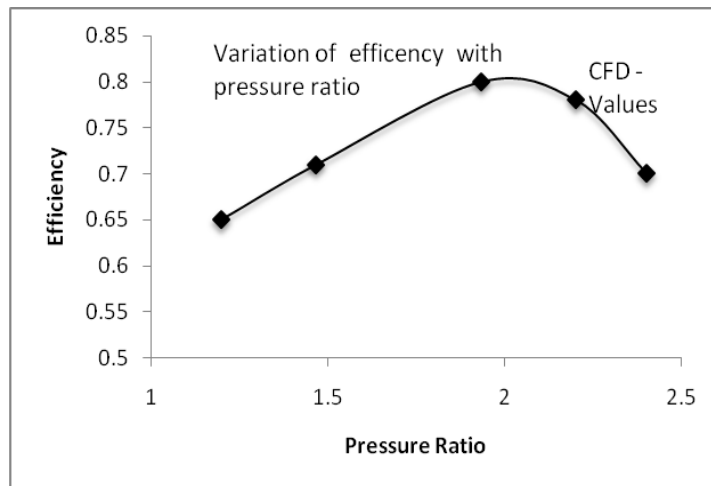**Figure 11.** Efficiencies vary with pressure Ratio

TABLE 3. Dimensionless performance parameters

S. No	Pressure Ratio	Efficiency
1	1.2	0.65
2	1.5	0.71
3	1.9	0.8
4	2.2	0.78
5	2.4	0.7

CONCLUSIONS

The meridional surface contours of the velocity vectors, or the Contour of Mass Averaged Pressure, are shown for turbine analysis. It is not taken into account that there are leaks. Analytical pressure, temperature, and entropy estimations at the turbine's inlet and outlet are more accurate than computational ones. Conclusions derived from this study include:

- The velocity of fluid at the input of the expansion turbine is 220 m/s, whereas the velocity at the turbine's outlet is 80 m/s. At the entry, the flow is recirculated and replenished. At the turbine's outlet, the flow shifted to the suction side. Analytical values are further removed from computational values. The velocity of the fluid at the intake of the expansion turbine is 210 m/s, whereas the exit velocity is 60 m/s. When compared to scenario 4, the output turbine velocity is lowered by 25%.
- In scenario 3, the entropy at the intake is 5330 J/kg.k and at the exit is 5410 J/kg.k. The greatest entropy in the blade-to-blade plane is 5420 J/kg.k at 20% of the blade passage from the entry, and as flow advances to the exit, the entropy steadily decreases. It's 5320 J/kg.k at intake and 5460 J/kg.k exit in instance 4. The highest entropy in the blade-to-blade plane is 5480 J/kg.k at 30% of blade passage from the entry, as is seen.
- Efficiency rises with pressure ratio up to a certain pressure ratio of design value, then declines as pressure ratio increases, according to computational efficiency values.

REFERENCES

1. Davydov, A. B., Kobulashvili, A. Sh. and Sherstyuk, A. N. The Design and Construction of Turboexpanders [Russian] Mashinostroenie, Moscow (1987).
2. Heinz P. Bloch. and Claire Soares Turboexpander and Process applications, Gulf Professional Publishing (2001).
3. Sixsmith, H. Miniature expansion turbines, C A Bailey (Ed), Advanced Cryogenics Plenum Press (1971), 225-243.
4. Izumi, H., Harada, S. and Matsubara, K. Development of small size Claude cycle helium refrigerator with micro turbo-expander Advances in Cryogenic Engineering (1986), V31, 811-818.
5. Sixsmith, H., Valenjuela, J. and Swift, W. L. Small Turbo-Brayton cryocoolers Advances in Cryogenic Engineering (1988), V34, 827-836.
6. Yang, K. J., He, H. B., Ke, G. and Li, G. Y. Application and test of miniature gas bearing turbines Advances in Cryogenic Engineering (1990), V35, 997-1003.
7. Davydenkov, I. A., Ravikorichy, Yu A., Davydov, A. B., Ermilov, Yu. I., Zakharova, N. E., Adler, Yu. R and Schedukhin Development of cryogenic turboexpanders with gas dynamic foil bearings Cryogenics (1992) 32 (Supplement) 80.
8. Aghai, R. R., Lin, M.C. and Ershaghi, B. High Performance cryogenic turboexpanders advances in Cryogenic Engineering (1996), V41, 941-947.
9. Aghai, R. R., Lin, M.C. and Ershaghi, B. Improvements of the efficiency of the turboexpanders in cryogenic applications Advances in Cryogenic Engineering (1996), V41, 933-940.
10. Mohammed Anees Sheik, Erdem Cuce, M K Aravindan, Abhishek Dasore, Upendra Rajak, Saboor Shaik, A Muthu Manokar, Saffa Riffat, A comprehensive review on recent advancements in cooling of solar photovoltaic (PV) systems using phase change materials (PCMs), *International Journal of Low-Carbon Technologies*, 2022;, ctac053, https://doi.org/10.1093/ijlct/ctac053
11. S.K. Mohammad Shareef, M Sai Vikas, A.L.N Arun Kumar, Abhishek Dasore, Sanjay Chhalotre, Upendra Rajak, Trikendra Nath Verma, Design and thermal analysis of engine cylinder fin body using various fin profiles, Materials Today: Proceedings, 47(17): 5776-5780 (2021).
12. Surendra, J., Rajyalakshmi, K., Apparao, B. V., Charankumar, G., & Dasore, A. Forecast and trend analysis of gold prices in India using auto regressive integrated moving average model. J. Math. Comput. Sci., 11(2), 1166-1175 (2021).
13. Dasore, A., Rajak, U., Panchal, M. et al. Prediction of Overall Characteristics of a Dual Fuel CI Engine Working on Low-Density Ethanol and Diesel Blends at Varying Compression Ratios. Arab J Sci Eng (2022). https://doi.org/10.1007/s13369-022-06625-8
14. Mitter, A., Jadeja, H. T. and Chakrabarty, H. D. Mechanical reliability and manufacturing process for indigenous development of turboexpander Proceedings of INCONCRYO-88 Indian Cryogenic Council (1988), 331-337.

15. Kumar, Ch Ashok, S. Udaya Bhaskar, and N. Srinivasa Rajneesh. "Fatigue analysis of four cylinder engine crank shaft." AIP Conference Proceedings. Vol. 2358. No. 1. AIP Publishing LLC, 2021.

16. Rajneesh, N. Srinivasa, et al. "Investigation on mechanical properties of composite for different proportion of natural fibres with epoxy resin." AIP Conference Proceedings. Vol. 2358. No. 1. AIP Publishing LLC, 2021.

17. Pavuluri, Subramanyam, et al. "Effect of reheating cycle on efficiency of Rankine cycle and its practical significance." AIP Conference Proceedings. Vol. 2358. No. 1. AIP Publishing LLC, 2021.

18. Rajneesh, N. Srinivasa, Ch Ashok Kumar, and S. Udaya Bhaskar. "Analysis of surface finish and residual stresses with shot peening on cylindrical specimens." Materials Today: Proceedings 44 (2021): 2606-2610

19. Subramanyam Pavuluri, B.Sidda Reddy, B.Durga Prasad, "An Experimental Investigation on the Performance, Combustion and Emission Characteristics of CI Diesel Engine at Various Compression Ratios with Different Ethanol-Biodiesel Blends", International Journal of Advanced Science and Technology, Vol. 29, No.5, pp. 2215-2226, 2020.

20. Santhi Priya, P., Pavuluri, S., Madaria, Y. (2022). Experimental Investigations of Process Variables on Wire Electrical Discharge Machining (WEDM) of AISI 52100 Steel. In: Chaurasiya, P.K., Singh, A., Verma, T.N., Rajak, U. (eds) Technology Innovation in Mechanical Engineering. Lecture Notes in Mechanical Engineering. Springer, Singapore. https://doi.org/10.1007/978-981-16-7909-4_53

21. Indrakanth, B., Udaya Bhaskar, S., Ashok Kumar, C., Srinivasa Rajneesh, N. (2022). Design and Optimization of Engine Block Using Gravity Analysis. In: Chaurasiya, P.K., Singh, A., Verma, T.N., Rajak, U. (eds) Technology Innovation in Mechanical Engineering. Lecture Notes in Mechanical Engineering. Springer, Singapore. https://doi.org/10.1007/978-981-16-7909-4_95

22. Subramanyam Pavuluri, Dr.B.Sidda Reddy, Dr.B.Durga Prasad. (2020). An Experimental Investigation on the Performance, Combustion and Emission Characteristics of CI Diesel Engine at Various Compression Ratios with Different Ethanol-Biodiesel Blends. International Journal of Advanced Science and Technology, 29(05), 2215-2226.

23. B. Sidda Reddy, A. Aruna Kumari, J. Suresh Kumar, K. Vijaya Kumar Reddy. Application Of Taguchi and Response Surface Methodology For Biodiesel Production From Alkali Catalysed Transesterification Of Waste Cooking Oil, International Journal of Applied Engineering Research, Vol. 4 (7), pp. 1169–1184, 2009.

24. B. Sidda Reddy, A. V. Hari Babu, S. Sreenivaslulu, K. Vijaya Kumar Reddy, Prediction of C. I. Engine Performance and NOX Emission Using CANFIS International Journal of Applied Engineering Research, Vol. 5 (5), pp. 763–778, 2010.

25. B. Sidda Reddy, J. Suresh Kumar and K. Vijaya Kumar Reddy, "Response Surface Methodology As A Predictive Tool For C. I Engine Performance and Exhaust Emissions of Methyl Esters of Mahua Oil", Journal on future Engineering & Technology, Vol.4, No.3, PP. 51-58, Februaryt-April2009. https://doi.org/10.26634/jfet.4.3.280